Journal of Low Temperature Physics, Vol. 93, Nos. 5/6, 1993

The Nucleation of Vortices in Superfluid ^{4}He: Answers and Questions

O. Avenel, G.G. Ihas† and E. Varoquaux*

Service de Physique de l'État Condensé, Centre d'Études de Saclay, 91191 Gif-sur-Yvette Cedex (France)

Laboratoire de Physique des Solides, Université Paris-Sud, Bât. 510, 91405 Orsay (France)

The velocity threshold for phase slips, v_c, has been measured in ultra-pure ^{4}He and ultra-dilute ^{3}He-^{4}He mixtures, down to a temperature of 15 mK. These experiments have revealed a crossover from a temperature-dependent régime above $\sim$ 150 mK to a plateau of v_c below in ultra-pure ^{4}He. Concentrations of ^{3}He impurities as low as a few parts in 10^{-9} greatly affect the plateau régime, causing v_c to decrease markedly at low temperature. These observations are interpreted in the framework of the nucleation, either thermally activated or by quantum tunnelling, of vortices in the approximate shape of half-rings. These vortices form on wall asperities at local velocities u_s estimated to be $\sim$ 22 m/s in these experiments. The half-ring model is shown to yield a critical velocity of the same magnitude but leaves many basic questions unanswered.

PACS numbers: 67 40 Hf, 67.40 Vs.

The existence of vortices in superfluid ^{4}He was postulated by Onsager, and independently by Feynman[1] who also suggested that they could account for the phenomenon of a critical velocity in superfluid flows. A large body of work has been devoted to their studies[2] as they constitute the archetypal defect of fluid dynamics. None the less, the formation of vorticity in superfluids is one of the fundamental remaining problems. Progress has been made in two directions in recent years. The mechanism for the onset of self-sustaining tangles has been extensively studied, both experimentally[3] and by numerical simulations.[4,5] The other direction which

†Permanent address: Center for Ultra-Low Temperature Research, Williamson Hall, University of Florida, Gainesville - FL 32611 - USA

0022-2291/93/1200-1031$07.00/0

has been explored lies in the observation of events involving single, or few, vortices in the critical superfluid flow through orifices of submicronic sizes.[6,7]

In this paper we report recent experiments on phase slippage in ultra-pure ^{4}He down to 15 mK from which we have inferred the existence of a quantum nucleation régime for vortices. Also, the study of the effect of minute amounts of ^{3}He impurities has led to an estimate of the local superfluid velocity at the nucleation site in our particular experiment.

The measurements are made using a two-hole, superfluid filled, hydromechanical resonator which has been described in detail elsewhere (see ref.[6] for references therein). One wall of this Helmholtz-type resonator is a flexible membrane which is driven to excite fluid flow through the resonator openings, one of which is a microscopic orifice. Fluid motion is observed by monitoring the membrane displacement with an ultra-sensitive superconducting sensor.

The validity of our observations relies on the absence of interferences from mechanical vibrations. We therefore describe in the first section the improvements in the experimental set-up and procedures that were carried out to decrease the likelihood of instrumental artifacts. We then turn to the purification of ^{4}He and the manufacture of the ultradilute ^{3}He-^{4}He samples, which play an important role in the interpretation of the experiments.

The next section is devoted to the experimental observations, namely the existence of a low temperature plateau for the critical velocity and the profound influence that minute traces of ^{3}He impurities have on the low temperature end of the plateau.

Then follows the description of a nucleation model, based on the formation of microscopic vortex half-rings at the walls, which is shown to offer a framework for the interpretation of these data.

We have not attempted here to review the field in a systematic way as other contributions to these Proceedings[8] cover the same topic. The present paper is basically a follow-up of the work presented at the Exeter meeting.[6] Some questions raised then have now found answers owing to new experimental results. These results have been reported previously.[9–11]

1. APPARATUS and EXPERIMENTAL TECHNIQUES

1.1. Vibration Isolation and Checks

For the quantum phase slips to be useful as a probe of vortex nucleation mechanisms, one must be able to observe slips which are due to intrinsic mechanisms. Previous work[12,13,6,14,15] showed that above $T = 150$ mK thermally activated processes dominated slip production. A deviation from this dependence was seen at lower temperatures when large amounts of ^{3}He impurities were present in the ^{4}He sample in the resonator. Various tests at both Orsay[16] and Berkeley[17] led to the conclusion that mechanical vibrations impinging on the cryostat were very likely causing phase slips at low temperature, imitating the thermal activation at higher temperatures. In order to minimize the effect of vibrations, a unique apparatus had to be designed and constructed in a new location at Saclay for the detection of intrinsically triggered phase slips.

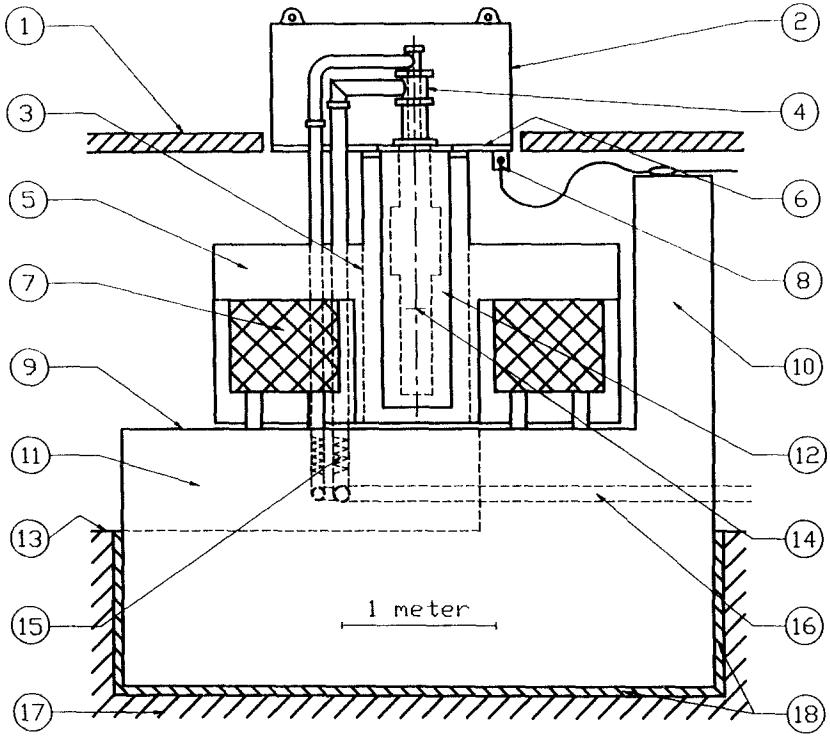

Fig. 1. Side projection view of apparatus. (1) Operation room floor; (2) Sound-proofing and rf enclosure; (3) Aluminium casing imbedded in concrete table; (4) Rotary seals for pumping lines; (5) 15-ton stainless steel reinforced concrete table; (6) Composite plate to complete enclosure # 2; (7) Air mounts; (8) rf filter box for electrical signals and power; (9) 45-ton concrete base; (10) Concrete pillar attached to base # 9 for small plumbing and electrical cable anchors; (11) Access tunnel to casing # 3; (12) Dewar surrounded by mixture of sand and visco-elastic pebbles filling # 3; (13) Basement floor; (14) Experimental resonator; (15) Elbow bellows for pumping lines; refrigerator plumbing cast into base # 9; (17) Undisturbed, virgin soil; (18) Polyurethane foam surrounding base # 9.

The design philosophy was threefold: (1) decouple to the extent possible all vibrations seen by the cryostat while maintaining the ability of humans to work around it; (2) make the cryostat as massive as feasible so that the amplitude of any vibrations that are coupled to it will be greatly attenuated; and (3) place the resonator at the center of mass and motion of the "isolated" structure to again minimize its motion. These were accomplished by mounting the cryostat on a 15 ton concrete table which in turn floats on air mounts which sit on a 45 ton concrete base. The base is isolated from the laboratory building by soil and foam. All connections, mechanical and electrical, are made through one or more rigid anchors with compliant couplings (bellows or loops of wire or tubing). The main features of the cryostat support structure are shown in Fig.1. Numbers preceded by hash signs in the next four paragraphs refer to the figure.

This massive concrete base #9 sits on polyurethane foam #18[18] in virgin soil #17 beneath the basement #13 of the laboratory building, with the top of the cryostat protruding through the floor #1 above. In this way no vibrations from the building or activities of workers in the building are directly coupled to the support structure. In addition, all plumbing and electrical connections to the cryostat are anchored to a concrete pillar #10 which is an integral part of the base. All pumps are in an adjacent basement room, with the plumbing anchored to the intervening masonry wall through which it passes. Hence, between each pump and the cryostat there are two rigid anchors with three separate vibration isolating bellows systems. These bellows were tuned with strategically-placed lead pieces to avoid resonances. The large refrigerator pumping lines are isolated with bellows elbows #15. The force due to atmospheric pressure is balanced by a 1 meter long steel cable anchored to the base at 135 deg to the elbows. This provided a low-pass cut-off frequency of about 1 Hz.

The cryostat top plate #6 is a sandwiched layer composite of chromium-coated aluminium, compressed wood and visco-elastic polymer[19] which dampens shear modes. This acts as the base of the rf shield box #2 which encloses the top of the cryostat. All communication to the cryostat is made through this plate, which sits on a large aluminium casing #3 cast into the concrete table #5. The dewar #12 then hangs inside this tube, shielded from sound disturbances by a mixture of sand and sorbothane (visco-elastic pebbles).[20] The tube is coated with sound proofing where it is not embedded in concrete. The dewar is especially constructed to avoid loose or floppy parts. Radiation shields are held firmly in place by super-insulation.

Electronic cables go through filters #8 and, with small plumbing lines, are coiled and then anchored to the base pillar #10. The large plumbing lines go down into an access tunnel #11 in the base #9 and then connect to pipes which are cast into the base. At the top of the cryostat these large pumping lines are connected with rotating seals #4. In this way, the refrigerator insert and hence resonator may be rotated during operation to observe gyroscopic effects due to the earth's rotation (a subject of future work[21]).

The resonator #14 is near the center of mass of the table and nearly coincides with the center of suspension of the air mount-table system. With the four Barry Control[22] air legs and 15 ton table, a 0.8 Hz resonant frequency is achievable, although 2 Hz is typical. The 45 ton base #9—foam #18 system has a cut-off response of about 15 Hz. Various measurements using piezoelectric transducers

and Q-Flex[23] accelerometers verified the response and integrity of the vibration isolation during the construction phase of the project.

1.2. Manufacture of the Ultra-Dilute ^{3}He-^{4}He Mixtures

Earlier work[12,16,24] has shown that small amounts of ^{3}He dissolved in the liquid ^{4}He contained in the resonator have a profound effect on the temperature dependence of the resonator amplitude at which slips occur. Therefore, in order to further investigate this effect, ultra-pure ^{4}He had to be produced. By starting with pure ^{4}He, measured amounts of ^{3}He were then added to allow a quantitative measure of the effect of ^{3}He impurities on the slip amplitude and hence vortex nucleation rate. The initial ^{4}He was pure enough so that no ^{3}He effect was detected even at the lowest working temperature (15 mK).

In order to save time, a three step process was used to remove ^{3}He impurities from liquid ^{4}He. The steps were: (1) pumping on a storage Dewar of liquid helium for a long period of time to fractionally distill away the ^{3}He impurities; (2) then drawing the helium remaining in the storage Dewar through a heat-flush apparatus; and (3) finally re-pumping the resulting helium to fractionate away the remaining ^{3}He impurities. Although no systematic attempt was made to determine which of these steps produced the desired purification and whether there was recontamination of the purified gas in the gas handling plumbing, it was found that even the final pumping process had a measurable effect on the purity. The ^{3}He impurity level of the "pure" ^{4}He (0.81 ± 0.10 ppb) and the nominally pure ^{4}He (100 ± 6 ppb) used to make the very dilute mixtures was determined by the U.S. Bureau of Mines[25] (ppb = 1 part in 10^9).

The first step, pumping on the storage Dewar, was done for more than one week with the temperature in the Dewar kept below that of the superfluid (lambda) transition. The second step involved passing the liquid helium through a very simple heat-flush apparatus after the design of Hendry and McClintock.[26] The stainless steel heat flush tube was 9 mm inner diameter and 95 mm long, followed by a 25 mm long powdered rouge superleak packed (hammered) between two 2 mm thick stainless steel sintered plugs. Heaters and thermometers were attached with GE varnish to the outside of this tube, which was then soldered inside a larger tube which provided vacuum insulation when the device was inserted into the storage Dewar. This same inner tube was brought out the top of the larger tube at the top of the Dewar and connected to a clean manifold made of all new (not ^{3}He contaminated) fittings and valves.

The manifold consisted of storage volumes, leak detector and mechanical pump connections, and a charcoal dip stick (for cryo-pumping) which held about 10 atmosphere-liters of helium gas when at 4.2 K. A heater power of 0.04 watts produced a gas flow of 16 stp-liter/hour from the purifier. In order to avoid contamination from pump oil which may have seen nominally pure helium, the dip stick was used for handling all purified gases. Pumps which had never been used to pump liquid helium were used to clean the plumbing.

The purifier was operated as follows. First it was used to make "pure" helium, which turned out to contain about 15 ppb ^{3}He. Then this gas was used to flush out the experimental cell and plumbing which had been previously used with ^{3}He.[27] The

storage Dewar containing the purifier was pumped for over one week, maintained at a temperature below T_λ. The flush heater was then turned on and the apparatus run with a mechanical pump for about 12 hours, discarding the helium coming through the superleak. Then, the charcoal dip stick is used to collect purified gas. When the dip stick is warmed to store the pure gas in tanks, the mechanical pump is used to keep the heat flush going, insuring that ^{3}He does not migrate through the superleak.

We found it extremely important to use plumbing and pumps which had never been exposed to helium, and to have a purifier and experimental cell gas handling system completely separate from the refrigerator plumbing.

The very dilute mixtures of ^{3}He in ^{4}He were made by first emptying and flushing the cell several times with pure helium, and then partially filling it with a measured amount of the 100 ppb nominally pure helium. This was followed by enough pure helium to fill the cell, thereby insuring that all of the ^{3}He contaminated gas was pushed into the cell.

Care was taken to avoid filling the cell in a manner which produced unnecessary remnant vorticity, thereby trapping ^{3}He.[10] The cell was held above T_λ while being filled, and then slowly cooled through the λ transition. If the helium was quenched into a cold (below T_λ) cell, as much as the equivalent of 30 ppb of ^{3}He would be trapped. This could be released by warming the cell up to near T_λ (see ref.[10] for details).

1.3. Data Analysis

In the experiments reported here, which make use of the same double-hole resonator as in a number of previous experiments (see, *e.g.*, refs.[6,13,28]), the resonator membrane was subjected to a constant *ac*-drive and its peak deflection, as measured by the SQUID pickup coil, was recorded at each (positive and negative going) half-cycle. As the power input to the resonator, driven on resonance, is constant and small, the phase slips are resolved and their number per unit time is fixed on the average. Between slips, the peak amplitude A_p raises by an amount which is very nearly constant because mechanical losses in the resonator are very small. For the same reasons (of high Q factor and low drive level), the waveform of the membrane motion is very nearly sinusoïdal and the membrane peak velocity is taken as proportional to its peak amplitude.

The output of the peak detector is recorded over a time interval of about 20 minutes during which the temperature is kept constant. The recorded data, which comprises over 32000 elementary peak amplitude measurements, is then analyzed with the help of a computer in several steps as explained in ref.[29]. The following quantities are successively obtained: the mean effect of the drive, the size of a 2π slip in detector units, the state of quantum circulation of the superfluid loop formed by the two holes after each slip,[21,11] and the distribution of peak amplitudes at which slips occur from each quantum state.[6,16] From this information is computed the value of the bias in the loop,[28,29] the empirical ratio R of the hydraulic inductances of the two holes (that is, the ratio of the cross sectional area to the hydraulic length of the parallel channel divided by the same ratio for the small orifice), the value of the critical amplitude extrapolated at zero bias and the width of the probability

distribution of the critical amplitudes. A second pass of the analysis program is then performed, fixing the geometrical constant R at its most probable value for the given cool-down. All the data reported here have been collected in the course of a single, long duration cool-down.

In these experiments, $R = 3.9$, which means that a fraction 1/4.9 of the total flow in and out of the resonator traversed the small orifice at small flow rates. This value varies slightly from one cool-down to the next as the cell contamination changes, but stays constant during the same cool-down. The mean size of a 2π slip was, in detector units, 36.5 and the low temperature critical peak amplitude, 7000. These values varied during the cool-down as the displacement sensor bias current could not be kept absolutely constant. The displacement sensor sensitivity was calibrated by applying a known *dc*-voltage to the membrane capacitor and recording the *dc* response of the detector output. This calibration can be performed to an accuracy of about 1% which enables the comparison of various runs in terms of detector units to the same accuracy. However, as discussed in refs.[13,30], actual flow rates through the holes can be directly determined to about 30% at best, and critical velocities in the small orifice to about 300%, owing to an indeterminacy in the actual cross-sectional area of the micro-orifice. The critical phase difference[28] in these experiments was $39.1 \times 2\pi$, a value rather typical of the orifice used. Assuming a hydraulic length of the order of 1 μm,[13] the mean critical velocity through the orifice, v_c, is evaluated to be 3.9 m/s. Values of the same order of magnitude have been found by other workers[31,32] in comparable orifices.

2. CRITICAL VELOCITY MEASUREMENTS

2.1. The Plateau at Low Temperature

The temperature dependence of the critical amplitude, determined from the probability distribution as explained in the previous section, is plotted in Fig. 2 for ultra-pure ^{4}He ($x_3 \leq 0.9$ ppb). Above a temperature of 150 mK, the critical amplitude decreases as a near-linear function of T, being proportional to $1 - T/T_0$ with $T_0 \simeq 2.40$ K. This value checks well with that of previous runs.[6,12,24] This observed temperature dependence of v_c extending well below 1 K has been taken[12] as an indication that vortices of very small length are nucleated in the immediate proximity of walls by a thermally activated process.

The new feature shown in Fig.2, reported in ref.[9], is a plateau in v_c extending below 120 mK down to the lowest temperature reached of about 15 mK. This plateau was not identified in our previous work either because ^{3}He was present in large (parts in 10^6) amounts, or due to a lack of data on the ultra-pure ^{4}He run.[33]

Among the possible causes for the occurrence of this plateau are the three following experimental artifacts:

1) It might be due to the few remaining ^{3}He quasiparticles. This possibility is ruled out by the detailed study of the effect on v_c of ^{3}He impurities in the 10^{-9} range of concentration, to be described below.

2) It is also quite clear that the temperature of the ^{4}He sample in the experimental cell follows that of the thermometer and cools below 150 mK as shown by direct evidence, and also by the study of the effect of ^{3}He.

3) Before the plateau can be interpreted as signalling the take-over of quantum fluctuations at low temperature, other possible sources of fluctuations, mechanical or acoustic disturbances, must be ruled out. This is by no mean trivial and we have to rely on the experimental ground work on vibration isolation described above as well as on the fact that the intrinsic features of the data, the statistical width of the critical transition, the occurrence of multiple slips, and the value of A_c itself in extreme cases, reveal the existence of outside interferences when they are present, and settle to reproducible values when they are not.

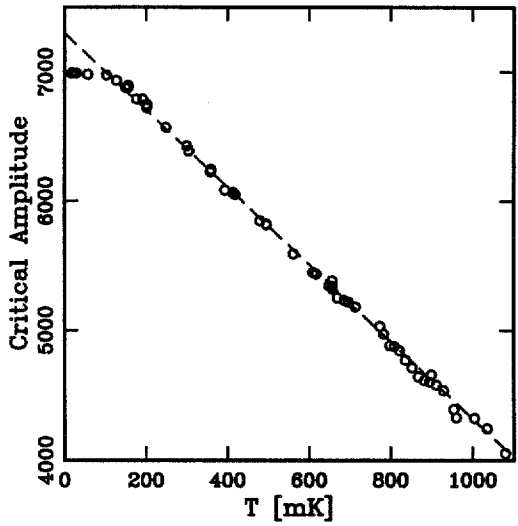

Fig. 2. Critical amplitude of the resonator membrane in pure ^{4}He (0.9 ppb ^{3}He) in detector units *vs* temperature. The dashed line is a linear fit to the data and extrapolates to zero at $T_0 = 2.45$ K. The data curve departs slightly from the linear fit as the temperature is lowered to approach the plateau.

We believe that none of these perturbing effects come into play in our experiments and that the observed plateau in v_c is an intrinsic feature. The observation of such a plateau has also been reported by Davis et al.[15] at about the same crossover temperature. This independent work strongly confirms our views that the effect is intrinsic. We note for further reference that the plateau is quite flat up to 120 mK and that the crossover region is sharply defined, indicating a rapid change from the high temperature régime to the low temperature régime. It is very unlikely that a takeover by mechanical vibration would be as sharply defined.

The width Δv_c of the critical transition also reflects, as shown in Fig.3, the same crossover from a temperature-dependent régime above 150 mK to a plateau below. The absolute value of Δv_c could be determined to about ± 10 % in quiet conditions, at off hours and long after helium transfers. This represents a marked improvement over our previous determination.[16]

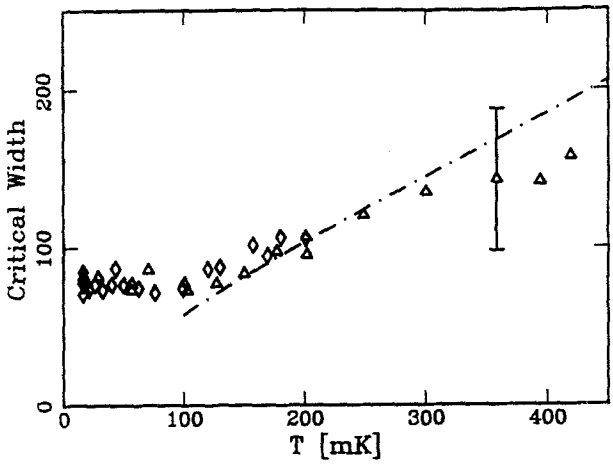

Fig. 3. Width of the phase slip critical transition (as defined in the text) in ultrapure ^{4}He in detector units *vs* temperature. The dashed curve is obtained from eq.(15).

2.2. The Effect of ^{3}He Impurities

Carefully monitored amounts of ^{3}He were added to the sample as described in section 1.2. The measurements were repeated and analyzed as those with ultra-pure ^{4}He. The results for six concentrations, ranging from 3 ppb to 100 ppb, together with those for the ultra-pure sample (nominally 0.9 ppb) are presented in Fig.4.[10] A sudden drop in v_c occurs at low temperature. This drop takes place at a temperature T_3 which can be seen to increase with concentration. The critical width Δv_c has been found to decrease below T_3, as shown in Fig.5, indicating a profound alteration of the nucleation process.[16,34]

3. THE HALF-RING MODEL

3.1. A Simple Estimate of the Energy Barrier

If the idea that vortices are nucleated and that the plateau in v_c is due to quantum fluctuations is accepted, then we can relate the vortex nucleation problem to that of a fairly general class of metastable systems, namely to that of a particle confined in a cubic potential well. This idealized case has been extensively studied over the past years, see *e.g.*[35–37] and we reap a crop of results which are nearly model-independent because cubic potentials (or more exactly cubic-plus-parabolic confining wells) can be mapped to most situations.

We have used this approach[9,11] to firstly obtain the attempt frequency $\omega_0/2\pi$ in terms of the observed crossover temperature T_q *via* the relation

$$\omega_0/2\pi = k_B T_q/\hbar, \tag{1}$$

relation which is valid for quite general systems, even in the presence of

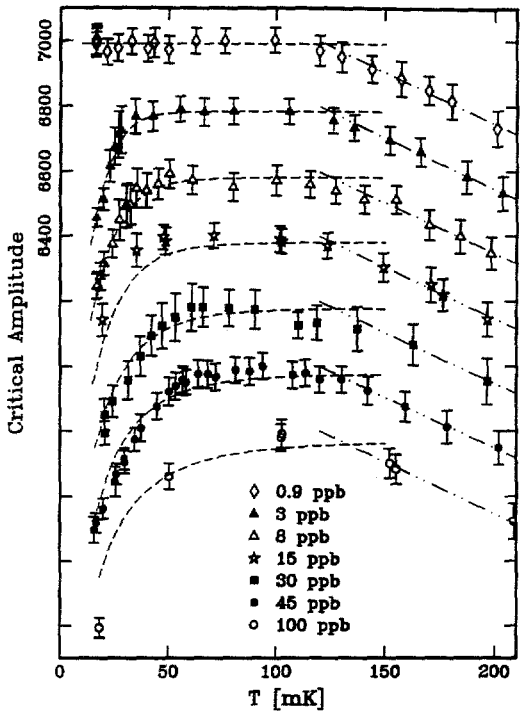

Fig. 4. Effect of ^{3}He impurities on the critical amplitude of the resonator *vs* temperature. Each symbol represents data on a sample of the ^{3}He impurity level shown. For clarity, data for each impure sample has been shifted down 200 detector units from the previous sample. Dash-dotted lines are linear fits to the thermal activation régime. The dashed curves are obtained as explained in §3.3.

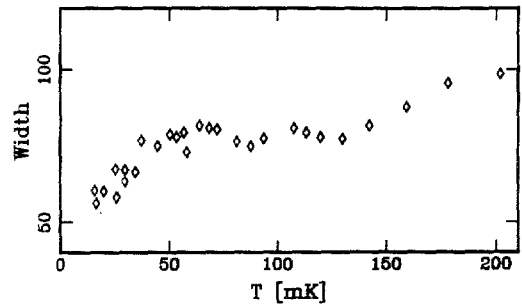

Fig. 5. Effect of ^{3}He impurities on the critical transition Δv_c *vs* temperature for the 45 ppb sample.

damping.[35–37] The corresponding value of the attempt frequency, $\omega_0/2\pi = 1.9 \times 10^{10}$ Hz for $T_g = 0.147$ K, is of a magnitude comparable to the natural frequency of vortices in this problem, noted by Muirhead, Vinen and Donnelly[38] to be the "cyclotron" frequency $\Omega_s = \kappa_4/\pi a_0^2$, κ_4 being the value of the quantum of circulation in ^{4}He. Taking the vortex core radius a_0 equal to 1 Å yields $\Omega_s/2\pi = 5 \times 10^{11}$ Hz, but, as discussed below, the value of a_0 close to walls where ω_0 need be evaluated is likely to be sizably larger than 1 Å.

Secondly, very close to the lability point, *i.e.* very close to the velocity u_c0 at which the confining potential vanishes, the energy barrier can be expressed in a general way as:

$$E_a = \frac{2}{3} E_J (1 - {u_s}^2/{u_{c0}}^2)^{3/2}, \tag{2}$$

u_s being the local superfluid velocity and u_{c0} being the value of u_s for which E_a vanishes. If we proceed to compute the critical velocity u_c and perform fits to the experimental data, *i.e.*, try to reproduce the slope of v_c *vs* T in Fig.2, we find[9,11] $E_J \sim 50$ K and $u_c/u_{c0} \sim 0.903$ on the low temperature plateau. This approach which, as already mentioned, does not rely on the details of a specific model, leads to a value of the energy barrier E_a on the plateau of 2.6 K. A check on the soundness of this general approach is that, as discussed below, it yields the observed critical width Δv_c with the values of ω_0 and u_c/u_{c0} determined from the slope of v_c *vs* T.

3.2. Half-Ring Model

Any specific model for the nucleation of vortices will have to reproduce the same results, and furthermore, provide a basis for the understanding of the ^{3}He effect described in section 2.2. The work of Muirhead *et al.*[38,39] which successfully accounts for negative ion propagation in liquid helium, provide an example of such a nucleation model. In particular, these authors have shown that the nucleation of a small vortex half-loop on the equator of a propagating ion is more probable than that of a full vortex loop encircling the ion. For wall nucleation over an asperity, the nucleation of small half-rings has been first considered by Volovik,[40] and then by Sonin.[41] This last author, following earlier work,[42,43] has also attempted to take into account the influence of the wall on the vortex energy. This question is a crucial one as a number of effects are expected to take place.

Firstly, the presence of a rigid boundary depletes ρ_s over a healing length which, in static conditions, has been evaluated by Hills and Roberts[44,45] to be about 2.1 Å at zero temperature and pressure. A number of experiments close to T_λ and involving low frequency second sound[46] and fourth sound,[47] as well as high frequency first sound[48] support the Hills-Roberts theory of the healing length, as discussed by Glaberson and Donnelly.[45]

Next, when the superfluid is set into motion with a velocity v_s, the healing length is expected to increase, at least in the framework of the Ginzburg-Pitaeskii[49,50] and the Gross-Pitaevskii[51–53]theories. Further complications come from the fact that walls are neither smooth[54,55] nor chemically inert.[56] Also, the superfluid develops a coarse-grained structure over a few atomic layers from the wall,[57] which in principle defeats approaches which treat it as a continuum. Finally, a vorticity layer of a few Ångströms in thickness may develop in the vicinity of rigid boundaries, as discussed by a number of authors.[40,41,43,58]

This last effect, found by considering solutions of the Gross-Pitaevskii (GP) equation involving vortices close to walls as will be discussed below, can be seen to arise in the following manner. It is known that the superfluid wavefuction amplitude, which is killed at a rigid boundary, heals back to its bulk value as $\tanh(z/\sqrt{2}a_0)$, z being the distance from the boundary and a_0 the GP coherence length. At the wall, the condensation energy has been lost, giving rise to a contribution to surface tension[59,60] which involves the square of the wavefunction gradient. The presence of a vortex decreases the value of the gradient, hence the surface tension. The kinetic contribution to the vortex energy is small as ρ_s is depressed, and energy is gained by the reduction in surface tension. The balance is such that it costs no energy to form vortices very close to a rigid boundary and a vortex layer of a few Ångströms in thickness develops. A similar proposition based on entirely different considerations has been put forward by G.A. Williams.[61] This vorticity layer may provide an explanation for the anomalously low contribution of the order parameter to surface tension discussed by Sobyanin and Stratonnikov[62] and also for the anomalously large vortex core sizes in films found by Kotsubo and Williams.[63]

This vorticity layer, real or virtual, constitutes the reservoir from which fluctuations extract vortices, pull them over (thermal case) or through (quantum case) the energy barrier confining the vorticity to the wall and let them escape to the superfluid bulk. Once nucleated and sufficiently far away from the wall, vortices move according to the laws of ideal fluid dynamics. In particular, they obey the Kelvin-Helmholtz theorem which states that vorticity is conserved in the fluid motion. Vortices are stable entities and can disappear only by a non-hydrodynamical process inverse of that of nucleation.

Before turning to the description of the nucleation process, let us mention a result obtained by Frisch *et al.*[64] which establishes that vortices are created, even in the absence of fluctuations, in a fluid governed by the GP equation, when the fluid local velocity past an obstacle exceeds the velocity of sound in the fluid. Vortices are created intermittently in lieu of shock waves developping into a sonic cone as in a classical compressible inviscid fluid.

Superfluid helium is a more complex fluid than the dilute Bose gas of the GP theory. It is not known which quantity replaces the GP sound velocity as setting the threshold for the hydrodynamical instability leading to the formation of vortices. It has however been revealed by ion propagation studies[65] that both rotons and vortices can be emitted by fast moving negative ions at different velocity thresholds. Thus, the two production mechanisms are different, that for rotons being set by the Landau criterion. If the proper velocity threshold for vortex formation cannot be directly inferred from the work of Frisch *et al.*, we shall still retain from it that vortices spontaneously appear at a certain maximum superfluid velocity, reached first close to the surface of obstacles.

These preliminaries have set the stage for the nucleation model, to which we now turn. We assume that vortices appear as half-rings extending perpendicularly to the wall in the vicinity of an asperity where the local superfluid velocity u_s is maximum. If we disregard healing of the wavefunction on the one hand and surface irregularities on the other, the formulation of the problem is quite simple. The energy E_0 and the impulse P_0 of a half-ring of radius R are just half of those of a full ring in the bulk:

$$E_0 = \frac{1}{4}\rho_s \kappa_4^2 R \eta, \tag{3}$$

$$P_0 = \frac{\pi}{2}\rho_s \kappa_4 R^2, \tag{4}$$

with $\eta = \ln(8R/e^2 a_0) = \ln(R/b)$ with $b = a_0/1.083$. Although we do not really need to consider vortices with radii smaller than b, the core parameter, we shall make the energy regular at small R by redefining η as $1/2\ln(1 + R^2/b^2)$.

By the same token, we find that the self-velocity of the vortex, taken as

$$v_v = \frac{\partial E_0}{\partial P_0} = \frac{\kappa_4}{4\pi R}\left\{\frac{1}{2}\ln(1 + \frac{R^2}{b^2}) + \frac{R^2}{R^2 + b^2}\right\}, \tag{5}$$

also becomes regular and tends to zero as $R \to 0$, thus accounting for the vorticity layer the existence of which we have assumed.

The nucleation problem is then treated in the same manner as by Langer and Reppy.[66] When placed in a homogeneous superfluid velocity field u_s with its impulse P_0 opposing the field, the vortex energy is reduced according to

$$E_v = E_0 - P_0 u_s = \frac{1}{4}\rho_s \kappa_4^2 \left\{\frac{1}{2}R\ln(1 + \frac{R^2}{b^2}) - \frac{2\pi}{\kappa_4}u_s R^2\right\}. \tag{6}$$

We introduce reduced units, lengths being in units of b, energies in units of $E^* = \rho_s \kappa_4^2 b$ and velocities in units of $v^* = \kappa_4/4\pi b$. In these reduced units and with $\varrho = R/b$, eqs.(5) and (6) now read:

$$\nu_v = \frac{v_v}{v^*} = \frac{1}{\varrho}\left\{\frac{1}{2}\ln(1 + \varrho^2) + \frac{\varrho^2}{1 + \varrho^2}\right\}, \tag{7}$$

$$\mathcal{E}_v = \frac{1}{8}\left\{\varrho\ln(1 + \varrho^2) - \nu\ \varrho^2\right\}. \tag{8}$$

The vortex reduced "free" energy $\mathcal{E}_v$ is plotted *versus* ϱ in Fig.6 for various values of the reduced superfluid velocity ν. It is seen to be a well-behaved confining potential for small half-rings. The activation energy $\mathcal{E}_a$ is found as a function of ν by looking for the maxima and minima of $\mathcal{E}_v$, whose locations for a given ν are solution of the following equation:

$$\frac{\partial \mathcal{E}_v}{\partial \varrho}|_\nu = 0 = \frac{\varrho}{4}(\nu_v - \nu). \tag{9}$$

The extrema of $\mathcal{E}_a$ are obtained for values of the half-ring radius such that the self-velocity ν_v exactly balances that of the applied flow field. The vortex self-velocity ν_v is plotted *versus* ϱ in Fig.6. Eq.(9) has two solutions, that is, $\mathcal{E}_a$ is well-defined for $\nu \leq \nu_m$, the maximum value of ν_v, which is equal to 0.432, reached for $\varrho_m = 1.258$. The quantities ν_m and ϱ_m characterize the lability point about which an expansion of $\mathcal{E}_a$ of the form given by Eq.(2) exists. Such an expansion is accurate for ν close to ν_m only, and it is necessary in practice to resort to a numerical evaluation of $\mathcal{E}_a(\nu)$.

Once the activation energy is known, the rate at which thermal activation of vortices takes place is given by Kramers' formula:[36,37]

$$\Gamma_{cl} = \frac{\omega_0}{2\pi} \exp\left\{-\frac{E_a(u_s)}{k_B T}\right\}, \tag{10}$$

the attempt frequency being taken numerically from Eq.(1). In principle, ω_0 can be obtained from the shape of the confining potential if the mass of the "particle" trapped in the well is known. It can be checked that if we take for this mass the mass displaced by the hollow core of the nucleated vortex, we obtain a reasonable order of magnitude for ω_0. However, not much confidence can be placed in the accuracy of such an evaluation as neither the shape of $\mathcal{E}_v$ close to $\varrho = 0$ nor the equivalent mass of the proto-vortex trapped at the wall is really well known. In that respect, the evaluation of T_q, which in turn yields ω_0, performed by Packard and Vitale[67] cannot be considered as reliable.

Below T_q, quantum fluctuations take over abruptly and the $T = 0$ nucleation rate is given by[35–37]

$$\Gamma_q = \frac{\omega_0}{2\pi}\left(864\pi\frac{E_a}{\hbar\omega_0}\right)^{\frac{1}{2}} \exp\left\{-\frac{36}{5}\frac{E_a}{\hbar\omega_0}\left[1+\frac{45\zeta(3)}{2\pi^3\omega_0\tau}\right]\right\}, \tag{11}$$

where the term proportional to $(\omega_0\tau)^{-1}$ expresses the contribution of damping to first order. As already mentioned, the plateau is quite flat and its onset abrupt, which implies that damping is negligible in the present problem. The crossover region about T_q has been studied in detail and, although no analytic result is available, the rate can still be evaluated.[68]

The nucleation rate in turn yields the probability that an event has taken place in the time interval $0 - t_f$:

$$p = 1 - \exp\left\{-\int_0^{t_f} \Gamma(u_s)dt\right\}. \tag{12}$$

In the following, t_f will be taken as half the resonator period. The probability, eq.(12), is an abrupt function of u_s, being negligible nearly up to the critical value and rising very rapidly to unity over a very narrow span of velocity. The critical value u_c is defined as that for which $p = 1/2$. The calculation of p can be carried out explicitly over a half-cycle of the resonator motion taking the expansion for E_a given by Eq.(2).[11] In this case, the asymptotic approximation of the integral in Eq.(12) yields:

$$p = 1 - \exp\left\{-\frac{\omega_0 t_f}{\pi}\left[\frac{k_B T}{6\pi E_a}\frac{\epsilon^2}{(1-\epsilon^2)}\right]^{\frac{1}{2}} \exp\left\{-\frac{E_a}{k_B T}\right\}\right\}, \tag{13}$$

where $\epsilon = (1 - {u_s}^2/{u_{c0}}^2)^{\frac{1}{2}}$ and $E_a = \frac{2}{3}E_J\epsilon^3$ are evaluated for $u_s = u_p$, the peak amplitude of the velocity. The local critical velocity u_c in this approximation is given by:

$$u_c = u_{c0}\left\{1 - \left[\frac{3}{2}\frac{k_B T}{E_J}\gamma\right]^{\frac{2}{3}}\right\}^{\frac{1}{2}}, \tag{14}$$

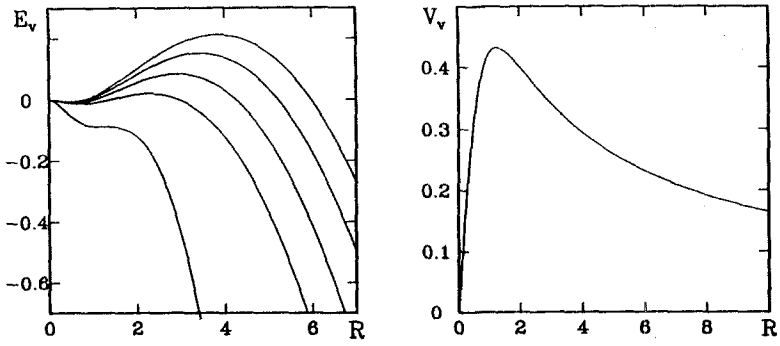

Fig. 6. Energy barrier E_v and vortex self-velocity v_v *vs* R in the simple half-ring model. The various energy barriers are for the following reduced superfluid flow velocities ν of (top to bottom) 0.308, 0.320, 0.347, 0.385 and $\nu_{c0} = 0.432$. These values of ν correspond to temperatures of 2.17, 1, 0.5, 0.147 and 0 K respectively (no fluctuation assumed at absolute zero) with $b = 9.44$ Å.

with

$$\gamma = \ln\left\{\frac{1}{\ln 2}\frac{\omega_0 t_f}{\pi}\left[\frac{k_B T}{6\pi E_a}\frac{\epsilon^2}{(1-\epsilon^2)}\right]^{\frac{1}{2}}\right\}.$$

If we evaluate γ in the vicinity of T_q, with $t_f = 40$ ms, $E_J = 50$ K and $u_p/u_{c0} = 0.9$, we find, again to logarithmic accuracy, $\gamma \simeq \ln(0.1\omega_0 t_f/\pi) = 18.8$. This procedure, outlined in refs.[6,11,16], yields the proper definition of the quantity Γ_{obs} introduced in ref.[12] as the inverse of the time necessary to detect a phase slip, a quantity which is instrumental in nature.

The width of the critical transition, defined[6,11,16] by $\Delta u_c = \partial u_p/\partial p$ evaluated at $p = 1/2$, is likewise found to be

$$\frac{\Delta u_c}{u_{c0}} = \frac{4}{\ln 2}\frac{(1-\epsilon^2)^{1/2}\epsilon^2}{1+6\gamma-3\epsilon^2(1+2\gamma)}. \tag{15}$$

Results (14) and (15) hold only for ϵ small. When this is not the case, at high temperature, or even close to T_q for higher accuracy, the calculations have to be carried out numerically. It may be mentioned here that these calculations have been checked by generating surrogate data from a program which simulates the operation of the cell.[69] The slip nucleation was treated as a random event with a probability given by eq.(10) and a given choice of Γ. The synthetized data were analyzed as if it were real data[29] and the values of v_c and Δv_c corresponding to the choice of Γ were obtained, establishing the consistency of the entire chain of operations.

To express the results, a value must be chosen for b, which is the only parameter in the model which can be varied to take into account the various phenomena that

we expect to take place close to walls. In view of Fig.6, this parameter can be thought of as fixing the distance from the wall at which the self-velocity of vortex half-rings start to decrease owing to the wall proximity. It also determines the energy scale through E^* and can be considered as fixing the energy, hence the length, of the nucleated vortex. In ref.[9], it has been found that the value $b = 9.44$ Å closely reproduces the temperature dependence of u_c from 0.15 to 1.9 K. It must be noted, however, that the fit relies explicitly on the temperature dependences chosen for $\rho_s(T)$[70] and a_0.[45] The corresponding local value of the critical velocity on the plateau is 6.5 m/s. A reasonable fit to the temperature slope of u_c is still obtained with a lower value of b, yielding $v_c \sim 12$ m/s on the plateau.

Probable values of the local critical velocity u_c at low temperature are discussed in ref.[6] and are thought to be in the range of 11 to 21 m/s. From the analysis of the effect of ^{3}He on the critical velocity, there is reason to think that the upper of these two values is the more likely. Hence, the value of 6.5 m/s obtained from the fit to the slope of $v_c(T)$ seems too low, probably due to the oversimplifications of the half-ring model described in this section, which limit the validity of quantitative evaluations.

3.3. ^{3}He Quasiparticles as Velocity Probes

We now turn to the analysis of the effect of ^{3}He quasiparticles on the low temperature behaviour of the critical velocity. As discussed in ref.[12], such an effect is also seen on film transfer and on ion propagation, which indicates that, also in these processes, vortices are nucleated with a rate which is rather strongly affected by the presence of ^{3}He.

We note first of all that, in the present case even more so than in ion propagation,[65,71] a quite large drop of v_c, of more than 15 %, is caused by a really minute concentration of impurities: at $x_3 = 3$ ppb, the mean distance between ^{3}He quasiparticles is 2500 Å, while the width of the slit is ~ 3000 Å and its length ~ 2000 Å. It is hardly conceivable that so dilute a gas can have such a marked effect unless the quasiparticles are trapped or collect in the vicinity of the nucleation site. This seems to be the case as indicated by the following first-level analysis of the data.

Let us provisionally define T_3 as the intersect of straight lines fit to the plateau and the low temperature portions of the data. A plot of $1/T_3$ *vs* $\ln x_3$, as shown in Fig.8, yields a straight line

$$\ln x_3 = \ln x_c - \Delta E_3 / k_B T_3, \tag{16}$$

with $\Delta E_3 = 0.16$ K and $x_c = 0.9$ ppm. Such a Arrhenius plot indeed suggests that ^{3}He quasiparticles collect in a potential well ΔE_3 when the temperature is decreased until their local concentration reaches x_c and their effect on v_c is felt. The distance between nearest neighbours decreases exponentially as the temperature is lowered below T_3, which explains why the nucleation process of Ångström size vortices can possibly be affected.

At first sight, it seems possible that the vorticity layer whose existence we have postulated forms a trap for ^{3}He. The binding energy of ^{3}He to vortex cores in the superfluid bulk is estimated[39,72] to be about 2.7 K. However, this is unlikely for

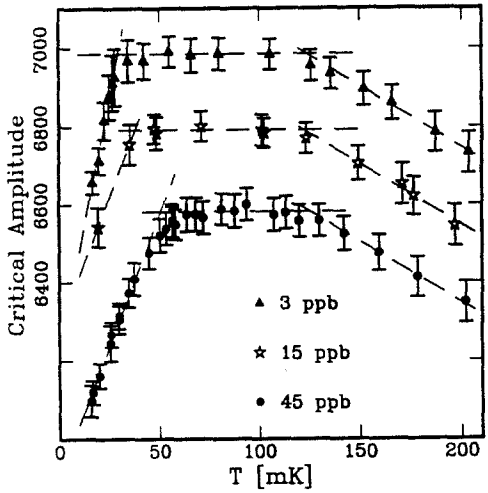

Fig. 7. T_3, as used in the text, is defined as the intersection of the linear fits to the plateau and the low temperature fall of the critical amplitude v_c *vs* T curves, as illustrated here for 3 concentrations. Data curves are shifted downward for clarity as in Fig.4.

two reasons. Firstly, the ^{3}He atoms are effectively pushed away from the walls by the ^{4}He atoms which are more attracted by the van der Waals forces, owing to their smaller atomic volume. There may exist cases where this general behaviour does not take place, as suggested by Pavloff and Treiner[57] and where ^{3}He bound states would exist close to the substrate. Such ^{3}He *substrate* states are seen in this experiment not to form in the sintered copper heat-exchanger and are not expected[73] to form on the nickel foil which carries the orifice. A second reason for not having ^{3}He quasiparticles trapped on vortices close to the wall lies in the fact that the trapping energy is proportional to ρ_s and goes to zero at the wall.

If ^{3}He quasiparticles do not dwell spontaneously at walls, they will nonetheless be pulled in by the Bernoulli effect which is surely to take place in the vicinity of the nucleation site where the superfluid velocity is at a maximum. This effect arises because the local pressure in the fluid is depressed in regions of high flow velocity by $\Delta P = -\frac{1}{2}\rho_s u_s^2$, which amounts to one third of a Bar at 20 m/s with $\rho_s = 0.145$ g/cm^3. The change in the ^{3}He quasiparticle chemical potential at equilibrium is related to the pressure change by

$$\Delta\mu_3 = \int_P^{P+\Delta P} \frac{\partial\mu_3}{\partial P}\, dP = v_3\, \Delta P,$$

where v_3 is the ^{3}He volume of one atom in the bath which is related to the ^{4}He atomic volume v_4 by $v_3 = v_4(1 + \alpha_{BBP})$. The quantity α_{BBP} is the Bardeen-Baym-Pines parameter whose value at $P = 0$ is 0.28.[74] At low temperature in the

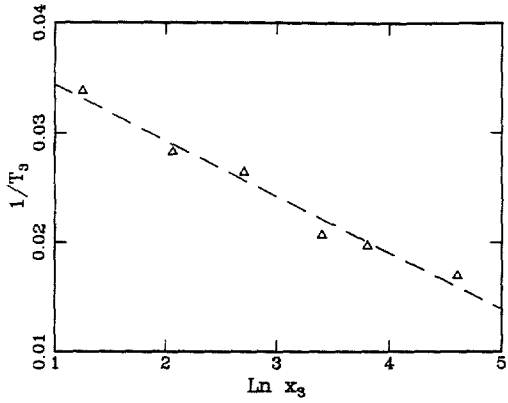

Fig. 8. Inverse of the temperature T_3, in mK, *vs* $\ln x_3$, the ^{3}He concentration x_3 in parts per 10^{-9}. The dashed line is the linear regression of the data.

bulk, $\rho_s = m_4/v_4$, m_4 being the ^{4}He bare mass, and we have finally:

$$\Delta\mu_3 = -\frac{1}{2}(1+\alpha_{BBP})\, m_4 u_s^2. \tag{17}$$

As discussed by Baym,[75] there exists another contribution to the quasiparticle energy change induced by the superfluid flow field u_s, arising from the difference between the bare (or inertial) mass m_3 and the effective mass m^* of the quasiparticle ($\sim 2.27 m_3$[74]). The backflow around the quasiparticle responsible for this difference directly interacts with the applied superflow and yields a contribution proportional to $1 - m_3/m^*$. The total energy change of the quasiparticle is expressed as a sum of the chemical potential difference and the effect of backflow:

$$\delta\epsilon = \frac{1}{2}\left[(1+\alpha_{BBP})\, m_4 + \left(1 - \frac{m_3}{m^*}\right) m_3\right] u_s^2. \tag{18}$$

The nucleation site, at which the local velocity u_s is at a maximum, acts as an atom trap for the quasiparticles into which they fall when the temperature is sufficiently low. The quasiparticle density n_3 at the nucleation site is related to that in quiescent regions of the cell, n_{30}, by[76]

$$n_3 = n_{30} \exp\{\delta\epsilon/k_B T\}, \tag{19}$$

even though the quasiparticle system is very far from thermal equilibrium. Eq.(19) can be compared directly with eq.(16). Eq.(18) for quasiparticle energy change will not hold close to the wall, but the local quasiparticle number density will not be much different from that given by eq.(19) a few healing lengths away.

The local density of quasiparticles at the nucleation site can thus become large enough so that the coincidence of a local fluctuation tending to form a nascent vortex and a quasiparticle is not an unlikely event. If we denote by V_n the volume in which the nucleation takes place, the probability to find one ^{3}He atom in this

volume (and one only) is $p_1 = n_3 V_n \exp\{-n_3 V_n\}$. More generally, the probability to find j ^{3}He atoms in V_n is $p_j = (n_3 V_n)^j \exp\{-n_3 V_n\}/j!$.

The energy barrier opposing nucleation is lowered by a quantity $\mathcal{L}_3 - E_k$ when one ^{3}He atom resides on the core, $E_k = \hbar^2/2m_3R^2$ being the zero point energy that the ^{3}He atom acquires when it is confined to the vortex core of a small half-ring of length R. The quantity $\mathcal{L}_3$ is a phenomenological parameter whose value can be expected to lie between the binding energy of a ^{3}He atom to a vortex in the bulk (*cir.* 2.7 K) and that close to a wall, which we have taken to be zero.

The half-ring nucleation rate for pure ^{4}He in the quantum régime, Γ_p, is given by eq.(11). With one ^{3}He present, the basic process of nucleation is the same, with the same attempt frequency, except that the energy barrier is now lowered in such a manner that the nucleation rate reads:

$$\Gamma_1 = \Gamma_p \exp\{36(\mathcal{L}_3 - E_k)/5\hbar\omega_0\}. \tag{20}$$

Likewise, in the presence of j ^{3}He atoms,[10] the rate increases according to $\Gamma_j = \Gamma_{j-1} \exp\{36(\mathcal{L}_3 - n^2 E_k)/5\hbar\omega_0\}$, with $n = j/2$ for even j and $n = (j+1)/2$ for odd j, assuming that the ^{3}He atoms trapped on the vortex core act as a one-dimensional ideal Fermi gas. This description is of course not expected to remain valid at large linear densities of ^{3}He on vortex cores.

The total nucleation rate is obtained by adding the rates of processes with $0, 1, \ldots, j, \ldots$ atoms multiplied by the probabilities p_j:

$$\Gamma = e^{-n_3 V_n} \Gamma_p + \sum_1^N p_j \Gamma_j, \tag{21}$$

N being the maximum number of ^{3}He atoms which can be closely packed on the half-ring at nucleation.

The critical velocity is then calculated as in §3.2. We have used in the calculations the limiting form of E_a given by eq.(2), with the same values of E_J, u_{c0} and ω_0 as previously, as our whole approach is valid only when the effect of ^{3}He is not too large.

The numerical determination of u_c involves four unknown parameters, $\delta\epsilon$, $\mathcal{L}_3$, E_k and V_n. In order to perform fits to the data, we must add another parameter which takes into account that some ^{3}He atoms, in concentration x_0, remain trapped at some locations in the cell and do not take part in the process affecting v_c. As discussed in ref.[10], of these five parameters, the first two have an exponentially strong influence on the results and are robustly determined: $\delta\epsilon = 0.204$ K, $\mathcal{L}_3 = 1.68$ K. For the other parameters, we find: $E_k = 0.4$ K, $V_n = (40)^3$ Å^3, and $x_0 = 1.5$ ppb. The calculated curves are shown in Fig.4.

The values of these parameters also account for the reduction in the critical width due to ^{3}He, shown in Fig.5. The nucleation rate is, in the presence of one ^{3}He, multiplied (as a first approximation) by the quantity $\exp\{36(\mathcal{L}_3 - E_k)/5\hbar\omega_0\}$, that is, it increases by a factor $\sim e^{10}$. For a coarse estimate, we may consider that this factor, which in reality reflects a modulation of the energy barrier by ^{3}He, can be included in the attempt frequency $\omega_0/2\pi$. It then increases the quantity γ entering eqs.(14) and (15) from 19 to 29, thereby reducing the width by about 30 %,[34] as observed (see Fig.5, *e.g.*).

The local value of the critical velocity u_c is found from $\delta\epsilon$, with the help of eq.(18), to be 22 m/s. The value of $\delta\epsilon$ can be compared to that of ΔE_3 found in the first-approach analysis outlined above. The difference of 20% between these two values, which translates into an indeterminacy of 10% on u_c, gives a measure of the influence of the model on the results. Apart from this weak dependence on the model, u_c is determined rather directly by the fact that the ultradilute ^{3}He impurities are attracted by a weak potential well at the nucleation site. It lies outside the range of 6 to 12 m/s found in §3.2 and could probably be affected by the presence of shallow bound states close to the substrate, if any, or by other manifestations of the van der Waals forces at the wall. Nonetheless, it is more reliable a value than those stemming out of the slope of $v_c(T)$, and which can themselves be also affected in an unknown way by wall proximity effects.

The value of $\mathcal{L}_3$ falls into the expected range, being about a half of that of the bulk. That of E_k corresponds to a half-ring radius at nucleation of 4.5 Å, assuming that the effective mass of the quasiparticle trapped on the core is close to the bare ^{3}He mass. This value of the radius is probably on the low side, as the classical vortex ring ($b \sim 1$ Å) with self-velocity $v_v = 22$ m/s has a radius of 12.8 Å. The value of the nucleation volume V_n which indicates over which typical size nucleation takes place (40 Å) is consistent with the radius of the nucleated half-ring, although it may be thought of as being on the high side. However, neither E_k nor V_n are very tightly fixed by the fit, nor is their physical meaning so exactly defined. We shall consider that the values found above for the model parameters are consistent with the overall picture for half-ring nucleation. There remains however a substantial discrepancy between the values of u_c found from the analysis of the effect of ^{3}He and from that of $v_c(T)$ in the previous section.

3.4. Walls and Vortices

In the following, we describe an attempt to tackle the question of the behaviour of a vortex close to an idealized wall, taken to be smooth and chemically inert, as this is one of the most serious shortcomings of the simple half-ring model outlined in §3.2 and 3.3. We use the framework of the Gross-Pitaevskii equation[51,52] which is known to provide a simple model of quantized vortices and which has already been used for such a purpose by Sonin[41] among others. In order to keep the problem simple, we only consider the case of a straight vortex filament extending perpendicularly from the wall to infinity in the z direction. This problem possesses axial symmetry about the vortex axis and we look for a solution to the GP equation of the form $\Psi_0 = e^{i\varphi} f(r,z)$ with $\nabla\varphi = 1/r$. The amplitude of the wavefunction f then satisfies the following equation:

$$\frac{\partial^2 f}{\partial r^2} + \frac{1}{r}\frac{\partial f}{\partial r} + \frac{\partial^2 f}{\partial z^2} + (1 - \frac{1}{r^2})f - f^3 = 0. \qquad (22)$$

The same reduced quantities as those of GP are used, namely, r and z are in units of the GP core parameter a_0, and f^2 is in units of ρ_s/m_4, the bulk superfluid number density. With these reduced quantities, f tends to 1 far from the wall and the vortex core. Its value at the wall and on the vortex core is taken to be zero. The asymptotic behaviour of $f(r,z)$ at large height z above the wall is the well-known GP solution for a vortex in the bulk[42,43,51,59,77,78] while at large radial distance r

from the vortex core, it can be shown to be given by:

$$f(r,z) = \left(1 - \frac{1}{r^2}\right)^{\frac{1}{2}} \tanh\left\{\left[\frac{1}{2}\left(1 - \frac{1}{r^2}\right)\right]^{\frac{1}{2}} z\right\}. \tag{23}$$

Eq.(23) tends as $r \to \infty$ toward the well-known $\tanh(z/\sqrt{2})$ solution in the absence of the vortex.

The boundary value problem is well-defined. We have looked numerically for the solution with the help of a Gauss-Seidel iteration scheme[79,80] on a 160 × 320 matrix for z varying from 0 to 10 and r varying from 0 to 20.

The quantity that we are ultimately interested in is the line energy $\delta E_0/\delta z$ of the vortex at height z which is obtained by taking the difference between the energies in the slab $z, z + \delta z$ with and without the vortex. These energies are calculated by integrating over r the thermodynamic potential density defined by[59,60]

$$\mathcal{F} = \{f^4 - 2f^2(1 - (\nabla\varphi)^2) + 2(\nabla f)^2\}. \tag{24}$$

At large r, the line energy $\delta E_0/\delta z$ behaves as $\tanh^2(z/\sqrt{2})\ln(r/a_0) + L_0$, the logarithmic divergence reflecting the behaviour of the fluid velocity at large distance which decreases as $1/r$ only. The quantity L_0 which comes out of the calculation is plotted in Fig.9 for a cut-off at $r = 20$.[81] It is seen to tend towards the value of the core energy of the GP vortex, 0.38, at large distance z from the wall. Close to the wall, it becomes negative and also diverges logarithmically with r, as can be seen directly from eq.(23). Vortices by walls cost little or no energy to form. The origin of this effect has been discussed in terms of a reduction of the surface tension at the beginning of §3.2.[58] This finding suggests that there should exist at walls a vorticity layer, but the definite structure of this layer would be known only if the appropriate solution of the GP equation were found. From the results shown in Fig.9, it seems as if its thickness could be of the order of 3 a_0, possibly increasing with applied velocity field.

Vortex nucleation, which takes place in the immediate vicinity of walls, is going to be affected by the negative value of $L_0(z)$ at small z. We proceed to estimate the change on v_c brought about by this result in the following manner. We compute the energy of the half-ring by assuming that it is made up of two straight filaments of the kind considered above, of length $\pi r/2$. The impulse of the half-ring is simply expressed by[41,82]

$$P_0 = \int dS \rho_s \kappa_4 f^2, \tag{25}$$

the integral being taken over the flat surface spanned by the half-ring and limited by the wall. The outcome of the integration over z (=r) is shown in Fig.9[83] where it is seen that P_0 also is strongly affected by walls: it reaches two-thirds of its asymptotic value above $5a_0$ only. The calculation of u_c then proceeds in the same manner as in §3.2, except that the energy barrier is now counted from the top of the vortex band ($E = 0$), assumed to be filled.

The calculated critical velocity on the quantum nucleation plateau is found to be 21 m/s and the radius of the nucleated vortex, 14 Å. The calculated temperature dependence is shown in Fig.10 for a value of the core parameter, b, of 4.5 Å, which

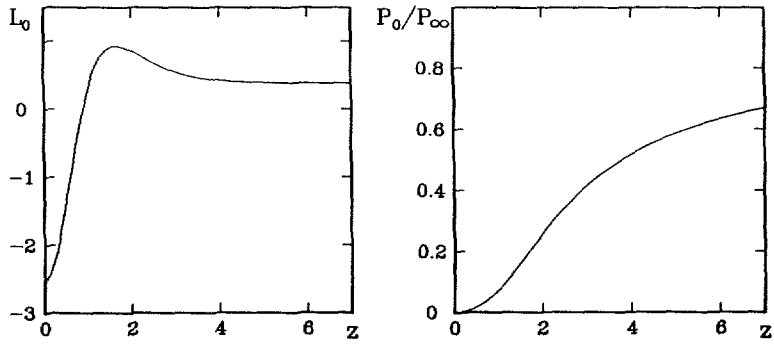

Fig. 9. Line energy L_0 of the straight filament and impulse of the half-ring P_0 at height z, normalized to its value at ∞ given by eq.(4), as computed from the solution to the Gross-Pitaevskii equation discussed in the text. The distance from the wall, z, is in units of a_0.

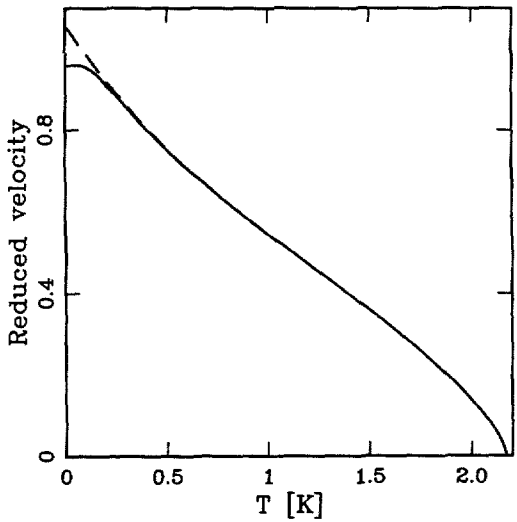

Fig. 10. Reduced velocity u_c/u_{c0} *vs* T computed from L_0 and P_0 as discussed in the text.

yields a fair representation of the slope of $v_c(T)$ up to 1.9 K.[58] Thus, we both obtain better agreement with the experimental results and improve the consistency of the half-ring model.

4. Answers and Questions

We have addressed here, among other things, some of the puzzling points raised at the NATO Workshop held in Exeter in 1990,[6] namely 1) the universal character of the $1-T/T_0$ dependence of v_c, 2) the apparent non-existence of a quantum plateau in flows through orifices, although such a plateau was observed in ion propagation studies. Both puzzles have now received answers. In addition, the study of the ^{3}He effect on v_c has provided us with important information on the nature of the binding of ^{3}He to vortex lines and on the value of the superfluid flow velocity at the site at which nucleation occurs.

The quasi-linear dependence of v_c on T (point 1 above) arises from the interplay of three factors:

1) The straightforward application of Kramers' formula in the vicinity of a lability point results, through eq.(14), in a temperature dependence going as $1-(T/\Theta)^{2/3}$ for $T \leq 0.5$ K. The considerations of §3.4 which lead to the assumption that a vortex *band* exists by the wall modify slightly this T-dependence since activation takes place from the top of the band.

2) The quantum corrections at low temperature amount, to lowest order in $1/T$, to adding a term in the exponent of Kramers' formula:[68]

$$\Gamma = \frac{\omega_0}{2\pi} \exp\left\{ -\frac{E_a(u_s)}{k_B T} + \frac{1}{12}\left(\frac{2\pi T_q}{T}\right)^2 \right\}.$$

The competition between quantum and thermal fluctuations starts to depress v_c at temperatures as high as $2\pi T_q \sim 0.9$ K and the effect is large at T_q.[68]

3) The high temperature end, close to the λ point, is dominated by the fact that the critical velocity is proportional to $\rho_s(T)/T$ as in the Iordanskii-Langer-Fisher theory (ILF).[66]

This can be shown in precisely the same way as in ref.[66] with the following outcome

$$v_c = \frac{{\kappa_4}^3}{32\pi} \frac{\rho_s(T)}{\gamma k_B T}(\eta^2 - 1).$$

Since half rings are nucleated, this expression is algebraically one-half of ILF, but the value of γ is twice as large in ILF:[66] homogeneous nucleation is a bulk effect and the number of possible nucleation sites is extremely large while wall nucleation takes place at one, or possibly a few, nucleation sites. Hence, the critical velocities for half-ring wall nucleation and full-ring homogeneous nucleation are similar, not surprisingly, but nucleation takes place at the wall where superfluid velocities are always higher.

The combination of these three effects results in the v_c *vs* T curve shown in fig. 10 for a value of b of 4.55 Å. Smaller values of b yield a more pronounced curvature at low temperature. So, unlike phase slips by 2π which are universal features and

do not depend of the peculiarities of a specific experimental situation, the quasi-linear T-dependence of v_c, the value of T_0, and the crossover temperature T_q are allowed, in the half-ring model, to vary slightly, reflecting local differences between nucleation sites.

On dimensional grounds, ω_0 is expected to vary as b^{-1}. Variations of b thus induce inverse variations of T_q and u_c. The observation at Berkeley[15] of a crossover temperature T_q about 40% higher than the value reported here , to which corresponds a value of T_0 smaller by roughly the same amount implies a b value of 3.3 Å and $u_c \sim 30$ m/s in the Berkeley experiments. Work with negative ions[65] resulted in a propagation velocity of 59 m/s which was taken to correspond to $b \simeq 1.5$ Å, values which scale well with the ones reported here. However, the crossover temperature T_q does not, which indicates that the ion surface acts on the superfluid wavefunction quite differently from solid walls.

Arguments based on a simple solution of the Gross-Pitaevskii equation have been put forward which show that the energy of vortices close to solid boundaries tends to a negative limiting value at the boundary, favouring the formation of a vorticity layer whose net effect is to increase the healing length. The value of b of 4.55 Å which was found to account for the slope of v_c *vs* T thus appears plausible. This observation, as well as the fact that realistic trajectories for the nucleated vortex can be found,[8,58,84,85] following earlier suggestions,[13,86] brings further support to the idea that half-rings form at the wall and evolve from there to cross the entire flow pattern.

There are, however, so many questions left unanswered in this work that detailed quantitative agreement between model and experiment is not expected. Among these questions, some are conceptual, like the full treatment of the vortex-at-wall problem and the related description of the simultaneous emission of rotons and vortices by superfluid flowing at high speed past an obstacle, or of the transition from 2-D to 3-D behaviour in vortex nucleation, *i.e.* from the Kosterlitz-Thouless kind of vortex pair unbinding to half-ring nucleation in full 3-D.[61] Other questions must be answered experimentally, the most important one being probably put by the onset, under certain ill-defined circumstances, of slips by multiples of 2π[6,13,31,32,87,88] which cannot be explained in terms of the nucleation of statistically independent events.[69]

ACKNOWLEDGMENTS

This work owes a great deal to the friendly assistance of many of our colleagues at Laboratoire de Physique des Solides (Orsay) and Service de Physique de l'État Condensé (Saclay), notably Michel Devoret, Daniel Estève, Marc Rouff and Heinz Schultz. We also wish to thank R. Aarts and R. Salmelin for their help in the setting-up of the experiment. M. Guille (C.E. Saclay) and D. Emerson (US Bureau of Mines) are particularly acknowledged for their fine mass spectroscopic analysis of the samples. The manuscript has benefitted from numerous suggestions from É. Sonin. One of us (GGI) is extremely grateful for the kind hospitality of the CE-Saclay.

REFERENCES

1. R.P. Feynman, in *Prog. Low Temp. Phys.*, Vol. 1, ed. C.J. Gorter (North-Holland, Amsterdam, 1955) p.17.
2. see, for a review, R.J. Donnelly, *Quantized Vortices in Helium* II (C.U.P., Cambridge, 1991).
3. J.T. Tough, in *Prog. Low Temp. Phys.*, ed. D.F. Brewer (North-Holland, Amsterdam, 1982), Vol. 3, p.133.
4. K.W. Schwarz, Phys. Rev. B 38, 2398 (1988).
5. R. Aarts, Ph.D. Thesis (Eindhoven University, 1993), unpublished.
6. E. Varoquaux, W. Zimmermann, Jr, O. Avenel, in *Excitations in Two-Dimensional and Three-Dimensional Quantum Fluids*, eds A.F.G. Wyatt, H.J. Lauter, Plenum, New-York (1991) p. 343.
7. R.M. Bowley, J. Low Temp. Phys. 87, 137 (1992).
8. For a recent review, see E. Varoquaux and O. Avenel, presented at LT20.
9. G.G. Ihas, O. Avenel, R. Aarts, R. Salmelin. E. Varoquaux, Phys. Rev. Lett. 69, 327 (1992).
10. E. Varoquaux, G.G. Ihas, O. Avenel, R. Aarts, Phys. Rev. Lett. 70, 2114 (1993).
11. E. Varoquaux, G.G. Ihas, O. Avenel, R. Aarts J. Low Temp. Phys. 89, 207 (1992).
12. E. Varoquaux, M.W. Meisel, O. Avenel, Phys. Rev. Lett. 57, 2291 (1986).
13. E. Varoquaux, O. Avenel, M. Meisel, Can. J. Phys. 65, 1377 (1987).
14. B.P. Beecken, W. Zimmermann, Jr., Phys. Rev. 35, 74 (1987).
15. J.C. Davis, J. Steinhauer, K. Schwab, Yu. Mukharsky, A. Amar, Y. Sasaki, R.E. Packard, Phys. Rev. Lett. 69, 323 (1992).
16. W. Zimmermann, Jr., O. Avenel, E. Varoquaux, Physica B 165&166, 749 (1990).
17. Ajay Amar, Ph.D. Thesis (University of California - Berkeley, 1992) unpublished.
18. Sylomer, from Getzner Chemie GmbH, Herrenau 5, A-6700 Bludenz-Bürs, Austria.
19. Dyad 601, Soundcoat, 1 Burt Drive, Deer Park, N.Y. 11729 - USA.
20. ENAC, 73, rue Noël-Pons - 92000 Nanterre - France.
21. E. Varoquaux, O. Avenel, G. Ihas, R. Salmelin, Physica B 178 (1992).
22. Model Al 133-15XX, Barry Controls GmbH Karl-Liebknecht-St. 30 - D-6096 Raunheim - Germany.
23. Models QA-700 and QA-900, Sundstrand Data Control, Redmont, WA 98052 - USA.
24. O. Avenel, E. Varoquaux, W. Zimmermann, Jr. Physica B 165&166, 751 (1990).
25. Bureau of Mines, US Dept. of the Interior, 1100 S. Filmore, Amarillo, TX 79101.
26. P.C. Hendry, P.V.E. McClintock, Cryogenics, 27, 131 (1987).
27. O. Avenel, E. Varoquaux, in *Quantum Fluids and Solids - 1989*, eds. G.G. Ihas, Y. Takano (AIP, NY, 1989), p. 3.
28. O. Avenel, E. Varoquaux, Jpn. J. Appl. Phys. 26, 1798 (1987).
29. R. Aarts, G.G. Ihas, O. Avenel, E. Varoquaux, presented at LT20 (Eugene - OR, 1993).
30. O. Avenel, E. Varoquaux, Phys. Rev. Lett. 55, 2704 (1985).
31. A. Amar, Y. Sasaki, R. Lozes, J.C. Davis, R.E. Packard, Phys. Rev. Lett. 68,

2624 (1992).
32. W. Zimmermann, Jr. J. Low Temp. Phys. 91, 219 (1993).
33. However, a plateau can be seen in fig.1 of ref.[12].
34. G.G. Ihas, O. Avenel, R. Aarts, E. Varoquaux, presented at LT20 (Eugene - OR, 1993).
35. A.O. Caldeira, A.J. Leggett, Ann. Phys. (N.Y.) 149, 374 (1983).
36. A. Larkin, K.K. Likharev, Yu.N. Ovchinnikov, Physica 126B, 414 (1984).
37. V.I. Mel'nikov, Phys. Reports 209, 1 (1991).
38. C.M. Muirhead, W.F. Vinen, R.J. Donnelly, Phil. Trans. Roy. Soc. A 311, 433 (1984).
39. C.M. Muirhead, W.F. Vinen, R.J. Donnelly, Proc. R. Soc. Lond. A 402, 225 (1985).
40. G. Volovik, Sov. Phys. JETP Lett. 15, 81 (1972).
41. E.B. Sonin, Sov. Phys. JETP 37, 494 (1973), Sov. Phys. Usp. 25, 409 (1982).
42. A.L. Fetter, Phys. Rev. 138, A429 (1965).
43. M.P. Kawatra, R.K. Pathria, Phys. Rev. 151, 132 (1966)
44. R.N. Hills, P.H. Roberts, J. Phys. C 11, 4485 (1978), P.H. Roberts, R.N. Hills, R.J. Donnelly, Phys. Lett. 70A, 437 (1979).
45. W.I. Glaberson, R.J. Donnelly, in *Prog. Low Temp. Phys.*, Vol. IX, ed. D.F. Brewer (Elsevier, Amsterdam, 1986) Ch.1.
46. G.G. Ihas, F. Pobell, Phys. Rev. A9, 1278 (1974).
47. W.Y. Tam, G. Ahlers, Phys. Lett. 92A, 445 (1982)
48. M.J. Lea, D.S. Spencer, P. Fozooni Phys. Rev. B 39, 6527 (1989).
49. V.L. Ginzburg, A.A. Sobyanin, Phys. Lett. 69A, 417 (1979), Sov. Phys. Usp. 19, 773 (1977), J. Low Temp. Phys. 49, 507 (1982) and Jpn. J. Appl. Phys. 26, 1785 (1987).
50. L.V. Kiknadze, Yu. G. Mamaladze, Sov. J. Low Temp. Phys. 17 156 (1991).
51. L.P. Pitaevskii, Sov. Phys. JETP 13, 451 (1961).
52. E.P. Gross, J. Math. Phys. 4, 195 (1963).
53. Yu. Mamaladze, O.D. Cheishvili, Sov. Phys. JETP 23, 112 (1966) and 25, 117 (1967).
54. Yu. Krasnov, Sov. J. Low Temp. Phys. 5, 519 (1979) and 6, 598 (1980)
55. M.W. Meisel, Pradeep Kumar, Physica B 165&166, 579 (1990).
56. S.I. Shevchenko, Sov. J. Low Temp. Phys. 9, 69 (1983) and 18, 223 (1992).
57. N. Pavloff, J. Treiner, J. Low Temp. Phys. 83, 331 (1991).
58. S. Burkhart, M. Bernard, O. Avenel, E. Varoquaux (submitted for publication).
59. V.L. Ginzburg, L.P. Pitaevskii, Sov. Phys. JETP 34, 858 (1958).
60. A.L. Fetter, J.D. Walecka, *Quantum Theory of Many-Particle Systems* (McGraw-Hill, N.Y., 1971), Ch. 13 and 14.
61. G.A. Williams, J. Low Temp. Phys. 89, 91 (1992).
62. A.A Sobyanin, A.A Stratonnikov, Sov. Phys. JETP Lett. 45, 613 (1987).
63. V. Kotsubo, G.A. Williams, Phys. Rev. B 33, 6106 (1986), G.A. Williams, Jpn. J. Appl. Phys. 26, 305 (1987).
64. T. Frisch, Y. Pomeau, S. Rica, Phys. Rev. Lett. 69, 1644 (1992), S. Rica, Y. Pomeau (private communication and to be published).
65. P.V.E. McClintock, R.M. Bowley, in *Excitations in Two Dimensional and Three Dimensional Quantum Fluids*, eds. A.F.G. Wyatt, H.J. Lauter, (Plenum, NY,

1991), p. 567.
66. J.S. Langer, J.D. Reppy, in *Prog. Low Temp. Phys.*, Vol. 6, ed. C.J. Gorter (North-Holland, Amsterdam, 1970) Ch. 1.
67. R.E. Packard, S. Vitale, Phys. Rev. 45, 2512 (1992).
68. H. Grabert, P. Olschowski, U. Weiss, Phys. Rev. B 36, 1931 (1987).
69. O. Avenel, R. Aarts, G.G. Ihas, E. Varoquaux, presented at LT20 (Eugene - OR, 1993).
70. J. Maynard, Phys. Rev. B 14, 3868 (1976).
71. P.C. Hendry, N.S. Lawson, P.V.E. McClintock, C.D.H. Williams, R.M. Bowley, Phil. Trans. R. Soc. London A 332, 387 (1990).
72. F. Dalfovo, Phys. Rev. B 46, 5482 (1992).
73. J. Treiner, private communication.
74. see, for instance, A. Ghozlan, E. Varoquaux, Ann. Phys. (Paris), 4, 239 (1979).
75. G. Baym, in *Mathematical Methods in Solid State and Superfluid Theory*, eds. R.C. Clark, G.H. Derrick (Oliver and Boyd Ltd, Edinburgh, 1969), p. 134, G. Baym, C. Ebner, Phys. Rev. 164, 235 (1967).
76. E.H. Kennard, *Kinetic Theory of Gases* (McGraw-Hill, NY, 1938), p. 77.
77. D. Amit, E.P. Gross, Phys. Rev. 145, 130 (1966).
78. V.L. Ginzburg, A.A. Sobyanin, Sov. Phys. JETP, 55, 455 (1982).
79. S.E. Koonin, *Computational Physics* (Addison-Wesley, 1986), Ch. 6.
80. W.H. Press, B.P. Flannery, S.A. Teukolsky, W.T. Vetterling, *Numerical Recipes* (CUP, Cambridge, 1986), Section 17.5.
81. The result for the line tension computed with a cut-off at $r = 20$ can be represented by $-2.5311 + 11.175Z^2 - 10.400Z^4 + 2.134Z^6$, with $Z = \tanh(z/\sqrt{2})$.
82. A. Fetter, in *The Physics of Liquid and Solid Helium*, eds. K.H. Benneman, J.B. Ketterson (Wiley, N.Y.,1976), part 1, Ch. 3.
83. The result for the impulse, normalized to its asymptotic value given by eq.(4) can be represented by $1 + 0.274/(1 + z^2/2) - (1.802/z)\tanh(z/\sqrt{2})$.
84. M. Bernard, S. Burkhart, O. Avenel, E. Varoquaux, presented at LT20 (Eugene - OR, 1993).
85. W. Zimmermann, Jr., this Meeting.
86. E. Varoquaux, O. Avenel, Physica Scripta, T19B, 445 (1987).
87. Ajay Amar, J.C. Davis, R.E. Packard, R.L. Lozes, Physica B 165&166, 753 (1990).
88. M. Bonaldi, M. Cerdonio, R. Dolesi, S. Vitale, presented at LT20 (Eugene - OR, 1993).